Contribution from the Department of Chemistry,
University of Delaware, Newark, Delaware 19716

Crystal Structures and $^1J_{Pt-P}$ Correlations for Trialkyl Phosphite–Platinum(II) Complexes: $[Pt[P(OMe)_3]_4](PF_6)_2$, $[Pt[P(OMe)_3]_3[P(O)(OMe)_2]]PF_6$, *cis*-$Pt[P(OMe)_3]_2[P(O)(OMe)_2]_2$, $[ClPt[P(OMe)_3]_3]PF_6$, and *cis*-$Cl_2Pt[P(OMe)_3]_2$

Q.-B. Bao, S. J. Geib, A. L. Rheingold, and T. B. Brill*

Received May 11, 1987

The first crystal structure determinations of trialkyl phosphite complexes of Pt(II) are reported along with those of mixed phosphite/phosphonate complexes. Crystal data: for $[Pt[P(OMe)_3]_4](PF_6)_2$, orthorhombic, *Pbca*, a = 21.495 (5) Å, b = 20.482 (6) Å, c = 15.495 (3) Å, V = 6822 Å^3, Z = 8; for $[Pt[P(OMe)_3]_3[P(O)(OMe)_2]]PF_6$, monoclinic, $C2/c$, a = 36.64 (1) Å, b = 8.298 (2) Å, c = 22.087 (6) Å, β = 120.93 (2)°, V = 5760 (3) Å^3, Z = 8; for *cis*-$Pt[P(OMe)_3]_2[P(O)(OMe)_2]_2$, monoclinic, $C2/c$, a = 13.26 (1) Å, b = 9.449 (7) Å, c = 19.16 (2) Å, β = 111.87°, V = 2229 (4) Å^3, Z = 4; for $[ClPt[P(OMe)_3]_3]PF_6$, monoclinic, $P2_1/n$, a = 7.776 (2) Å, b = 29.132 (6) Å, c = 11.435 (3) Å, β = 102.60 (2)°, V = 2528 (1) Å^3, Z = 4; for *cis*-$Cl_2Pt[P(OMe)_3]_2$, monoclinic, Cc, a = 6.904 (1) Å, b = 16.966 (3) Å, c = 13.523 (3) Å, β = 100.98 (1)°, V = 1555.0 (5) Å^3, Z = 4. The Pt(II)–phosphite bonds are shorter than the Pt(II)–phosphonate bonds. The distortion of these complexes away from idealized square-planar geometry toward tetrahedral or pyramidal arrangements of ligands is related to the cone angle of the ligands. The trans influence of the ligands is $P(O)(OMe)_2 > P(OMe)_3 \gg Cl$. There is a crude trend that higher values of $^1J_{Pt-P}$ from $^{31}P\{^1H\}$ NMR measurements correspond to shorter Pt–P bond distances in the 16 Pt–phosphite and Pt–phosphonate bonds structurally characterized to date.

Introduction

Few studies on platinum(II)–phosphite complexes have been undertaken.[1] The tendency of these complexes to dealkylate in the presence of nucleophiles and form phosphonate complexes reduces their tractability.[1-6] In fact, although the structures of several triphenyl phosphite–Pt(II) complexes are available,[7,8] no crystal structure determinations have been reported for trialkyl phosphite complexes of Pt(II). Unlike the alkyl analogues, the triphenyl phosphite ligand is essentially inert to nucleophilic attack, leading to an arylphosphonate. The structures of several Pt(II)–alkylphosphonate complexes, which are the stable products of dealkylation, have been reported.[9-12] This paper describes the structures of five trimethyl phosphite complexes of Pt(II). A comparison of the bond distances and angles about the Pt(II) center is made to establish the structural patterns for these compounds. Of particular interest is whether the Pt(II)–phosphonate and Pt(II)–phosphite bond distances track $^1J_{Pt-P}$ measured from ^{31}P NMR spectroscopy. A qualitative trend exists between these two parameters for Pt(II)–phosphine complexes[13,14] but has not been established for other phosphorus donor ligands. A trend was found, but the correlation is rather poor and certainly no better than that for Pt(II)–phosphine complexes.

Experimental Section

The compounds studied in this work were obtained as described previously.[1]

X-ray Data Collection. The parameters used during the collection and refinement of crystal data for compounds **1–5** are contained in Table I. Colorless crystals of each were attached to fine glass fibers with epoxy cement. On the basis of systematic absences, **1** and **4** were uniquely determined to crystallize in *Pbca* and $P2_1/n$, respectively; **2**, **3**, and **5** crystallize in either $C2/c$ or Cc. On the basis of E statistics and the successful solution and refinement of these structures, the centrosymmetric space group $C2/c$ was chosen for **2** and **3**, while the noncentrosymmetric space group Cc was chosen for **5**. Unit-cell dimensions were derived from the least-squares fit of the angular settings of 25 reflections with $20° < 2\theta < 30°$. Data for all five structures were empirically corrected for absorption. For **3** and **4**, a profile fitting procedure was applied to all intensity data to improve the precision of weak reflections.

Solution and Refinement of Structure. **1**, **3**, and **4** were solved via heavy-atom methods; **2** and **5** were solved by direct methods (SOLV). In each case, the Pt atom was located. The remaining non-hydrogen atoms were found from subsequent difference Fourier syntheses. All hydrogen atom positions were calculated [d(C–H) = 0.96 Å; thermal parameters equal to 1.2 times the isotropic equivalent for the carbon to which it was attached]. All non-hydrogen atoms were refined anisotropically for all five structures.

1 crystallizes with one $[Pt(P(OMe)_3)_4]^{2+}$ ion and two PF_6^- ions per asymmetric unit. P–F distances were tied to a common variable that refined to 1.513 (2) Å. The asymmetric unit of **2** contains one $[Pt[P(OMe)_3]_3[P(O)(OMe)_2]]^+$ ion and one PF_6^- ion. P–F distances, tied to a common variable, refined to 1.517 (3) Å. **3** contains a half-molecule of $Pt[P(OMe)_3]_2[P(O)(OMe)_2]_2$ per asymmetric unit with Pt residing on the 2-fold axis. **4** and **5** crystallize with one molecule of $[Pt[P(OMe)_3]_3Cl]PF_6$ and one of $Pt[P(OMe)_3]_2Cl_2$, respectively, per asymmetric unit. **4** contains a disordered methoxy group, with C(9) and O(9) at 56% occupancy, C(9′) and O(9′) at 44% occupancy. The PF_6^- ion in **4** was ordered with an average P–F distance of 1.50 (1) Å.

All examined specimens of **4** showed contributions to the diffraction pattern from either a satellite crystal or a twin. While various rejection criteria were employed to filter out spurious contributions, the high residuals and noisy background for **4** likely reflect a less than complete rejection of these contributions.

For all compounds, inspection of F_o vs F_c values and trends based on $\sin\theta$, Miller index, or parity group showed no systematic errors in the data. All computer programs used in the data collections and refinements are contained in the Nicolet program packages P3, SHELXTL (version 5.1), and XP (Niciolet XRD, Madison, WI).

Atomic coordinates for **1–5** are provided in Tables II–VI, respectively Selected bond distances and angles are provided in Tables VII and VIII. Additional crystallographic data are available as supplementary material.

Results and Discussion

Crystal Structure Determinations. Because our principal interest was the geometry about the Pt(II) center, only the bond distances and angles in this region are discussed. All other bond distances and angles were not especially noteworthy and are archived.

1. $[Pt[P(OMe)_3]_4](PF_6)_2$ (1) vs $[Pt(PEt_3)_4](ClO_4)_2$.[15] The cations in these complexes are isoelectronic. The $[Pt(PEt_3)_4]^{2+}$ ion is distorted toward tetrahedral geometry ($\angle PPtP \simeq 150°$) due to steric crowding of the ligands. However, the cone angle[16] of $P(OMe)_3$ (107 ± 2°) is smaller than that for PEt_3 (132 ± 2°), resulting in a relaxation of **1** (Figure 1) toward the preferred

(1) Bao, Q.-B.; Brill, T. B. *Inorg. Chem.*, preceding paper in this issue.
(2) Couch, D. A.; Robinson, S. D. *Inorg. Chim. Acta* **1974**, *9*, 39.
(3) Troitskaya, A. D.; Itskovich, T. B. *Tr. Kazan Khim.-Tekhnol. Inst.* **1953**, *18*, 59; *Chem. Abstr.* **1957**, *51*, 1148.
(4) King, C.; Roundhill, D. M. *Inorg. Chem.* **1986**, *25*, 2271.
(5) Mijamoto, T. *J. Organomet. Chem.* **1977**, *134*, 335.
(6) Solar, J. M.; Rogers, R. D.; Mason, W. R. *Inorg. Chem.* **1984**, *23*, 373.
(7) Caldwell, A. N.; Manojlovic-Muir, L.; Muir, K. W. *J. Chem. Soc., Dalton Trans.* **1977**, 2265.
(8) Albinati, A.; Pregosin, P. S.; Ruegger, H. *Inorg. Chem.* **1984**, *23*, 3223.
(9) Berry, D. E.; Bushnell, G. W.; Dixon, K. R. *Inorg. Chem.* **1982**, *21*, 957.
(10) Berry, D. E.; Bushnell, G. W.; Dixon, K. R.; Pidcock, A. *Inorg. Chem.* **1983**, *22*, 1961.
(11) Roundhill, S. G. N.; Roundhill, D. M. *Acta Crystallogr., Sect. B: Struct. Crystallogr. Cryst. Chem.* **1982**, *38*, 2479.
(12) Wagner, K. P.; Hess, R. W.; Treichel, P. M.; Calabrese, J. C. *Inorg. Chem.* **1975**, *14*, 1121.
(13) Mather, G. G.; Pidcock, A.; Rapsey, G. J. N. *J. Chem. Soc., Dalton Trans.* **1973**, 2095.
(14) Pidcock, A. *Adv. Chem. Ser.* **1982**, *No. 196*, 1.
(15) Kozelka, J.; Lüthi, H.-P.; Dubler, E. *Inorg. Chim. Acta* **1984**, *86*, 155.
(16) Tolman, C. A. *J. Am. Chem. Soc.* **1970**, *92*, 2956.

0020-1669/87/1326-3453$01.50/0

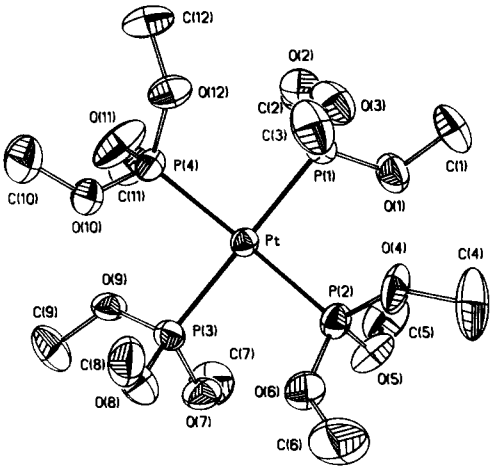

Figure 1. Structure of $[Pt[P(OMe)_3]_4]^{2+}$ in $Pt[P(OMe)_3]_4(PF_6)_2$ (**1**).

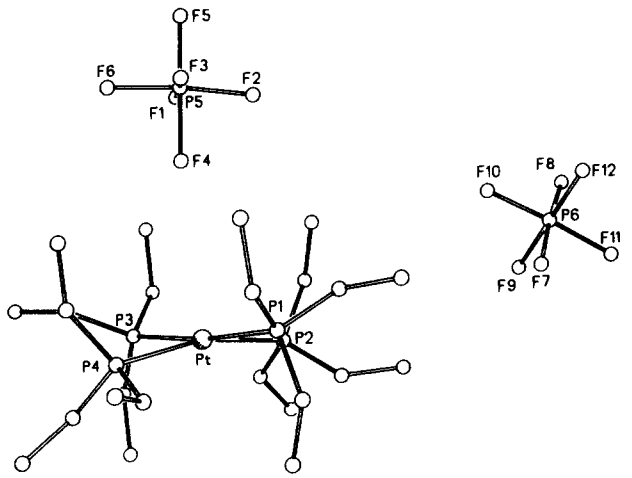

Figure 2. Relationship of the anion positions in $Pt[P(OMe)_3]_4(PF_6)_2$, showing that one of the PF_6^- ions shares a 4-fold axis with the cation.

square-planar geometry ($\angle PPtP \simeq 170°$). The deviation of the atoms from the least-squares plane is given in Table IX, revealing that the distortion remains toward a tetrahedral geometry. The distortion of **1** is further reduced to a $\angle PPtP$ of 174° when one of the $P(OMe)_3$ ligands is replaced by a still less sterically demanding Cl ligand to produce $[ClPt[P(OMe)_3]_3]^+$ ($\mathbf{4}^+$).

The average Pt–P bond distance in **1** (2.310 (4) Å) is less than that in $[Pt(PEt_3)_4]^{2+}$ (2.336 (7) Å) because the more electronegative substituents on P in **1** contract the phosphorus atom and enhance the Pt–P π back-donation. In addition, the larger steric demands when R = alkyl will lengthen the Pt–P bonds. This pattern of shortened $Pt-PR_3$ bonds when R = OMe compared to R = Me and Et is general to all of the compounds whose crystal structures have been investigated.

The arrangement of ions in the crystal lattice of **1** differs from the other salts. One of the PF_6^- ions is positioned so that the PF_6^- and $[Pt[P(OMe)_3]_4]^{2+}$ ions share a common 4-fold axis (Figure 2) . However, the Pt–F distance of 3.72 Å exceeds the sum of the van der Waals radii of Pt and F (3.2–3.4 Å).[17] C–H···F hydrogen bonding may contribute to the position of the PF_6^- ion relative to the cation.

2. $[Pt[P(OMe)_3]_3[P(O)(OMe)_2]]PF_6$ (2) and *cis*-$Pt[P(OMe)_3]_2[P(O)(OMe)_2]_2$ (3) Compared to 1. Demethylation of one of the $P(OMe)_3$ ligands of **1** yields **2** (Figure 3). The Pt–$P(O)(OMe)_2$ bond is slightly longer than the Pt–$P(OMe)_3$ bond (2.322 (3) vs 2.293 (3) Å), which is the same trend found for other complexes[18-20] and is in accordance with $[P(O)(OMe)_2]^-$ being a slightly weaker σ donor and/or π acceptor than $P(OMe)_3$. The Pt–$P(OMe)_3$ bond trans to the phosphonate is slightly longer than that trans to phosphite, but the difference is barely statistically significant. The ion is slightly distorted towards tetrahedral (Table IX) as evidenced by the average $\angle PPtP$ angle of 169°.

Double demethylation of **1** yields **3** (Figure 4). The quality of the diffraction data for **3** was worse than that for the other structures giving rise to somewhat larger esd's. **3** lies on a center of symmetry. The Pt–phosphite bonds (2.294 (9) Å) are shorter than the Pt–phosphonate bonds (2.33 (1) Å). The phosphoryl oxygen atoms are *exo* in the solid state. The ion is slightly distorted

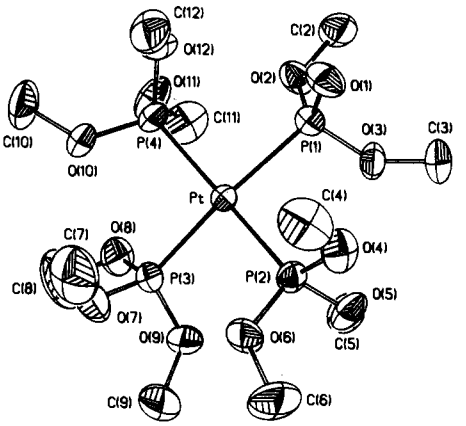

Figure 3. $[Pt[P(OMe)_3]_3[P(O)(OMe)_2]]^\bullet$ ion in $[Pt[P(OMe)_3]_3[P(O)(OMe)_2]]PF_6$ (**2**).

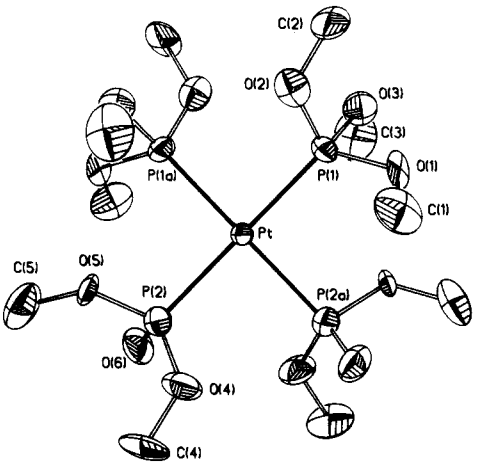

Figure 4. *cis*-$Pt[P(OMe)_3]_2[P(O)(OMe)_2]_2$ (**3**).

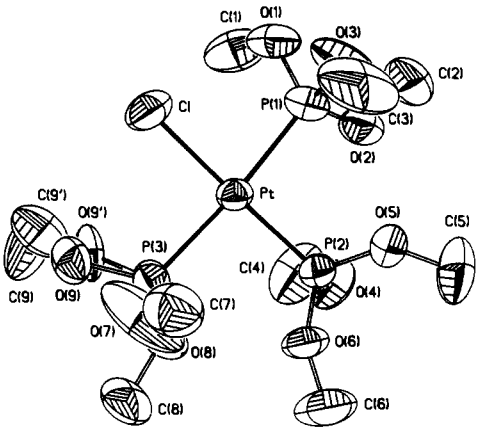

Figure 5. Structure of the cation in $[ClPt[P(OMe)_3]_3]PF_6$, (**4**).

(17) Bondi, A. *J. Phys. Chem.* **1964**, *68*, 441.
(18) Day, V. W.; Tavanaiepour, I.; Abdel-Meguid, S. S.; Kirner, J. F.; Goh, L.-Y.; Muetterties, E. L. *Inorg. Chem.* **1982**, *21*, 657.
(19) Towle, D. K.; Landon, S. J.; Brill, T. B.; Tulip, T. H. *Organometallics* **1982**, *1*, 295.
(20) Sullivan, R. J.; Bao, Q.-B.; Landon, S. J.; Rheingold, A. L.; Brill, T. B. *Inorg. Chim. Acta* **1986**, *111*, 19.

Table I. Crystal, Data Collection, and Refinement Parameters for **1–5**

	1	2	3	4	5
formula	$C_{12}H_{36}O_{12}P_6F_{12}Pt$	$C_{11}H_{33}O_{12}P_5F_6Pt$	$C_{10}H_{30}O_{12}P_4Pt$	$C_9H_{27}O_9P_4ClF_6Pt$	$C_6H_{18}O_6P_2Cl_2Pt$
cryst syst	orthorhombic	monoclinic	monoclinic	monoclinic	monoclinic
space group	*Pbca*	*C*2/*c*	*C*2/*c*	$P2_1/n$	*Cc*
a, Å	21.495 (5)	36.64 (1)	13.26 (1)	7.776 (2)	6.904 (1)
b, Å	20.482 (6)	8.298 (2)	9.449 (7)	29.132 (6)	16.966 (3)
c, Å	15.495 (3)	22.087 (6)	19.16 (2)	11.435 (3)	13.523 (3)
β, deg	90	120.93 (2)	111.87 (8)	102.60 (2)	100.98 (1)
V, Å^3	6822 (3)	5760 (3)	2229 (4)	2528 (1)	1555.0 (5)
Z	8	8	4	4	4
ρ(calcd), g cm^{-3}	1.91	1.89	1.97	1.96	2.20
μ, cm^{-1}	47.3	54.9	69.7	62.8	100.5
temp, °C	23	23	23	23	23
cryst dimens, mm	0.31 × 0.31 × 0.31	0.31 × 0.31 × 0.33	0.40 × 0.40 × 0.40	0.16 × 0.30 × 0.36	0.30 × 0.40 × 0.40
radiation	*a*	*a*	*a*	*a*	*a*
diffractometer	Nicolet R3m/μ	Nicolet R3m/μ	Nicolet R3m/μ	Nicolet R3m/μ	Nicolet R3m/μ
scan speed, deg min^{-1}	variable, 6–20	variable, 5–20	variable, 5–20	variable, 5–20	variable, 7–20
2θ scan range, deg	$4 < 2\theta < 50$	$4 < 2\theta < 50$	$4 < 2\theta < 44$	$4 < 2\theta < 50$	$4 < 2\theta < 60$
scan technique	Wyckoff	Wyckoff	$\theta/2\theta$	ω	Wyckoff
data collcd	$+h,+k,+l$	$\pm h,+k,+l$	$\pm h,+k,+l$	$\pm h,+k,+l$	$\pm h,+k,+l$
weighting factor, *g*	0.0010	0.0010	0.0013	0.0010	0.0010
no. of data read	6622	5602	1636	4792	2425
no. of unique data	6004	5067	1445	4450	2271
no. of unique data obsd	$3196 > 3\sigma(F_o)$	$3505 > 3\sigma(F_o)$	$926 > 3\sigma(F_o)$	$2916 > 5\sigma(F_o)$	$2034 > 5\sigma(F_o)$
std reflcns	3 std/197 reflcns	3 std/197 reflcns	3 std/197 reflcns	3 std/197 reflcns	3 std/197 reflcns
R_F, %	5.32	4.56	8.59	4.09	4.29
R_{wF}, %	5.15	4.53	8.53	4.45	4.65
GOF	1.174	1.133	1.569	1.102	1.068
maximum peak, e Å^{-3}	1.05 (near Pt)	0.71 (near F(6))	3.88 (near Pt)	0.67 (near F(2))	2.36 (near Pt)
data/param	3196 reflcns/389 least-squares params	3505 reflcns/317 least-squares params	926 reflcns/123 least-squares params	2916 reflcns/290 least-squares params	2034 reflcns/153 least-squares params
Δ/σ	0.041	0.016	0.004	0.136	0.032

[a] Graphite-monochromated Mo Kα; λ = 0.710 73 Å.

toward tetrahedral ($\angle$PPtP $\simeq$ 170°).

The structure of Pt[P(OH)(OMe)$_2$]$_2$[P(O)(OMe)$_2$]$_2$[6] has been determined. This complex is the diprotonated product of the quadruple Arbuzov reaction of **1**. All of the Pt–P bond distances are the same (2.312 (3) Å) within experimental error. Perhaps owing to the P–O···H···O–P hydrogen bonding, the PtP_4 framework achieves square-planar geometry within experimental error.

3. [ClPt[P(OMe)$_3$]$_3$]PF$_6$ (4) vs [ClPt(PMe$_3$)$_3$]Cl.[21] The smaller cone angle of P(OMe)$_3$ (107 ± 2°) compared to that of PMe$_3$ (118 ± 2°) leads to less distortion of **4** (Figure 5) from square-planar geometry than is observed for [ClPt(PMe$_3$)$_3$]$^+$. The average $\angle$PPtP is 174° in **4** compared to 166° in the phosphine complex. The shorter Pt–P bond distance for P(OMe)$_3$ trans to Cl (2.216 (3) Å) than that for P(OMe)$_3$ trans to another phosphite ligand (2.299 (3) Å) is consistent with the lower trans influence of Cl compared to P(OMe)$_3$. The Pt–Cl bond distance in **4** (2.333 (3) Å) is slightly shorter than that in [ClPt(PMe$_3$)$_3$]$^+$ (2.371 (3) Å), in accordance with the fact that PMe$_3$ has a larger trans influence than P(OMe)$_3$.[22]

4. *cis*-Cl$_2$Pt[P(OMe)$_3$]$_2$ (5). The formally equivalent Pt–P bonds of **5** (Figure 6) differ by 0.037 (3) Å, which markedly exceeds the differences for equivalent ligands in any of the other complexes. Surprisingly, there are no short intermolecular interactions in the crystal lattice that can account for the differences. The shortness of the Pt–P bonds is partly compensated for by the platinum atom through lengthening of the Pt–Cl bonds in **5** compared to those in **4**. **5** is also unusual in that while distortion of the ion from square-planar geometry is expected to be small based on the cone angles, the ClPtP angle of 174° is the result of a square pyramidal rather than a tetrahedral distortion. The Pt atom is displaced from the plane by 0.069 Å. There are no Pt to Cl intermolecular contacts less than 5.7 Å. Hence, compounds **1–4** display a tetrahedral distortion while **5** is pyramidal. The magnitude of the distortion appears to reflect the space

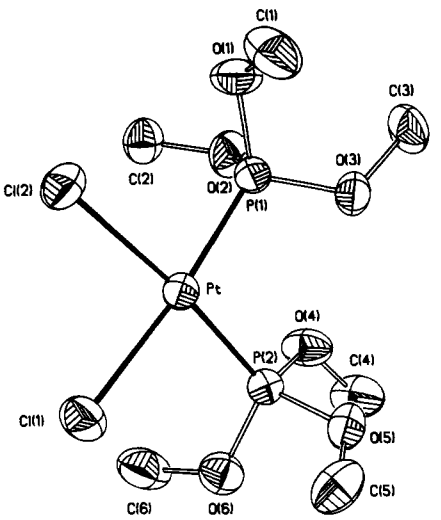

Figure 6. Structure of *cis*-Cl$_2$Pt[P(OMe)$_3$]$_2$, (**5**).

required by the ligands while the direction of the distortion is less easily predicted.

Correlation of $^1J_{Pt-P}$ and the Pt–P Bond Distance. A trend exists between $^1J_{Pt-P}$ and the Pt–P bond distances of Pt(II)–phosphine complexes.[13,14] Both parameters are partly sensitive to the s-orbital character in the bond. However, owing in part to the fact that several other molecular variables also contribute to $^1J_{Pt-P}$,[23] the correlation is not especially good.[14] Using the crystal structures in this paper and several from the literature,[6-12] the pattern of $^1J_{Pt-P}$ and the Pt–P bond distances is now analyzable for Pt–phosphite and Pt–phosphonate complexes. Table X lists the values of $^1J_{Pt-P}$ from the ^{31}P NMR spectra and the Pt–P bond distances. These data are plotted in Figure 7. As with the Pt–phosphine complexes it can be seen that only a qualitative trend exists. For

(21) Favez, R.; Roulet, R.; Pinkerton, A. A.; Schwarzenbach, D. *Inorg. Chem.* **1980**, *19*, 1356.
(22) Allen, F. H.; Sze, S. N. *J. Chem. Soc. A* **1971**, 2054.
(23) Pople, J. A.; Santry, D. P. *Mol. Phys.* **1964**, *8*, 1.

Table II. Atomic Coordinates (×10⁴) and Isotropic Thermal Parameters (Å² × 10³) for $C_{12}H_{36}O_{12}P_6F_{12}Pt$ (**1**)

	x	*y*	*z*	*U*[a]
Pt	1247.6 (3)	5815.4 (2)	7265.0 (3)	38.4 (2)
P(1)	699 (2)	6654 (2)	7913 (2)	52 (1)
P(2)	896 (2)	6128 (2)	5921 (2)	52 (1)
P(3)	1706 (2)	4902 (2)	6664 (2)	50 (1)
P(4)	1789 (2)	5653 (2)	8536 (2)	47 (1)
P(5)	−653 (2)	4310 (2)	8014 (3)	68 (2)
P(6)	−1603 (3)	7645 (2)	5106 (4)	104 (3)
F(1)	−541 (6)	3954 (7)	7170 (7)	165 (7)
F(2)	−985 (7)	4872 (7)	7570 (11)	230 (11)
F(3)	−732 (6)	4652 (5)	8881 (5)	152 (7)
F(4)	−67 (4)	4717 (4)	7841 (7)	142 (6)
F(5)	−1233 (5)	3924 (7)	8183 (8)	220 (9)
F(6)	−260 (5)	3806 (5)	8466 (10)	228 (11)
F(7)	−1178 (8)	7984 (8)	5750 (12)	270 (13)
F(8)	−2025 (9)	7356 (11)	4433 (10)	304 (14)
F(9)	−1047 (7)	7512 (7)	4529 (11)	318 (16)
F(10)	−1496 (9)	7005 (7)	5557 (14)	350 (18)
F(11)	−1667 (8)	8313 (5)	4696 (12)	298 (15)
F(12)	−2160 (7)	7778 (8)	5666 (11)	338 (17)
O(1)	83 (5)	6788 (5)	7392 (6)	72 (4)
O(2)	483 (4)	6546 (5)	8866 (6)	66 (4)
O(3)	1059 (5)	7309 (5)	8050 (7)	81 (5)
O(4)	839 (5)	6878 (5)	5858 (7)	80 (5)
O(5)	295 (5)	5822 (5)	5541 (6)	75 (4)
O(6)	1398 (5)	5925 (5)	5246 (6)	78 (5)
O(7)	1299 (5)	4532 (4)	5974 (6)	70 (4)
O(8)	2309 (4)	4980 (5)	6116 (7)	78 (4)
O(9)	1828 ()	4395 (4)	7406 (5)	58 (4)
O(10)	2466 (5)	5483 (5)	8296 (7)	80 (4)
O(11)	1589 (6)	5148 (6)	9204 (7)	110 (6)
O(12)	1826 (5)	6305 (4)	9054 (6)	64 (4)
C(1)	−337 (8)	7322 (8)	7587 (11)	102 (9)
C(2)	3 (7)	6112 (7)	9106 (10)	84 (7)
C(3)	1632 (8)	7476 (7)	7632 (11)	85 (7)
C(4)	440 (9)	7259 (8)	5337 (13)	122 (10)
C(5)	−248 (8)	5670 (8)	6009 (11)	105 (9)
C(6)	1551 (10)	6214 (10)	4487 (12)	127 (11)
C(7)	794 (8)	4130 (8)	6219 (12)	104 (9)
C(8)	2742 (7)	5484 (8)	6206 (11)	88 (8)
C(9)	2179 (8)	3793 (7)	7261 (11)	94 (8)
C(10)	2996 (8)	5520 (10)	8839 (13)	133 (10)
C(11)	1152 (7)	4665 (8)	9203 (10)	81 (7)
C(12)	1808 (8)	6387 (8)	9991 (9)	88 (8)

[a] Equivalent isotropic *U* defined as one-third of the trace of the orthogonalized U_{ij} tensor.

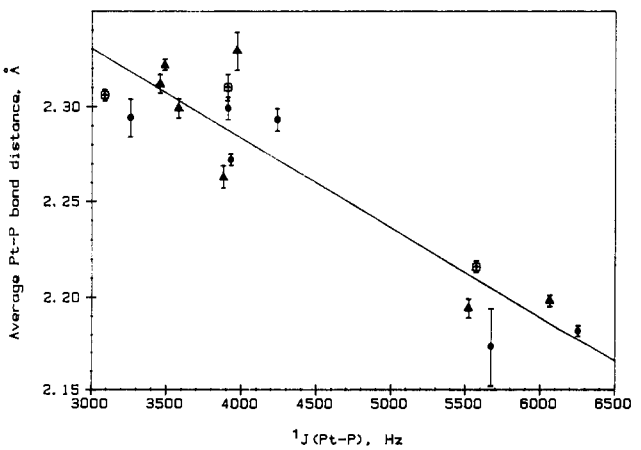

Figure 7. Qualitative trend of the average Pt–P bond distance vs. $^1J_{Pt-P}$ in Pt(II)–phosphite (●) and Pt(II)–phosphonate complexes (▲). The circled points (⊙) are for Pt–P bonds in which only the ligand trans to this bond has been changed. The error bars refer to the total range of bond distances for a given compound added to the esd for the most deviant bonds.

phosphite and phosphonate ligands trans to one another, there is a random clustering of the data in the 3000–4000-Hz and 2.27–2.33-Å region. It is the addition of data for phosphite and phosphonate groups trans to Cl that produces the qualitative trend.

Because many different types of complexes are included in Figure 7, it is worthwhile to focus on $^1J_{Pt-P}$ for the primed ligand in *trans*-Pt[P(OMe)$_3$]$_2$[P′(OMe)$_3$]X complexes, where X = Cl, P(OMe)$_3$, and P(O)(OMe)$_2$. These data points are circled in Figure 7. A good correlation might be expected for this series[24,25] because only the trans ligand is changed. On the contrary, for these three compounds, the correlation is no better than over the larger set of data.

The effect of ligand substitution on the chemical shift and coupling constants in analogous pairs of phosphite and phosphine

Table III. Atomic Coordinates (×10⁴) and Isotropic Thermal Parameters (Å² × 10³) for $C_{11}H_{33}O_{12}P_5F_6Pt$ (**2**)

	x	*y*	*z*	*U*[a]
Pt	1538.7 (1)	10056.0 (5)	2811.9 (2)	38.5 (1)
P(1)	2221 (1)	9074 (3)	3231 (1)	47 (1)
P(2)	1334 (1)	8837 (3)	1754 (1)	49 (1)
P(3)	900 (1)	11413 (4)	2333 (1)	55 (1)
P(4)	1712 (1)	10770 (4)	3933 (1)	51 (1)
P(5)	4400 (1)	1142 (3)	625 (2)	78 (2)
F(1)	4392 (2)	−647 (7)	762 (4)	157 (9)
F(2)	4413 (3)	2925 (7)	484 (4)	188 (11)
F(3)	4766 (4)	857 (8)	501 (9)	231 (14)
F(4)	4683 (4)	1432 (8)	1410 (3)	210 (10)
F(5)	4085 (4)	870 (8)	−155 (3)	226 (11)
F(6)	4022 (4)	1413 (8)	713 (9)	247 (14)
O(1)	2338 (2)	7412 (8)	3474 (4)	69 (4)
O(2)	2515 (2)	10369 (9)	3815 (4)	68 (4)
C(2)	2965 (4)	10321 (16)	4173 (6)	87 (7)
O(3)	2320 (2)	9504 (9)	2625 (4)	63 (4)
C(3)	2502 (4)	8474 (18)	2342 (7)	98 (9)
O(4)	1527 (2)	7101 (8)	1796 (4)	69 (4)
C(4)	1424 (5)	5836 (17)	2115 (8)	109 (10)
O(5)	1449 (3)	9616 (9)	1223 (4)	74 (4)
C(5)	1541 (4)	11280 (15)	1220 (6)	84 (8)
O(6)	843 (2)	8555 (10)	1359 (4)	75 (4)
C(6)	614 (4)	7871 (22)	657 (7)	129 (9)
O(7)	508 (3)	10577 (12)	2285 (5)	98 (6)
C(7)	500 (5)	9032 (21)	2532 (9)	134 (13)
O(8)	954 (3)	13031 (10)	2735 (4)	86 (5)
C(8)	633 (5)	13965 (23)	2741 (10)	171 (16)
O(9)	752 (2)	11981 (10)	1578 (4)	79 (4)
C(9)	335 (4)	12317 (25)	1038 (7)	152 (12)
O(10)	1285 (2)	10739 (10)	3939 (3)	64 (4)
C(10)	1251 (4)	11145 (49)	4542 (7)	103 (9)
O(11)	1932 (3)	12369 (10)	4266 (4)	86 (6)
C(11)	2041 (5)	13584 (14)	3970 (7)	103 (10)
O(12)	2022 (3)	9624 (10)	4558 (4)	74 (4)
C(12)	1919 (5)	7966 (16)	4559 (7)	100 (10)

[a] Equivalent isotropic *U* defined as one-third of the trace of the orthogonalized U_{ij} tensor.

Table IV. Atomic Coordinates (×10⁴) and Isotropic Thermal Parameters (Å² × 10³) for $C_{10}H_{30}O_{12}P_4Pt$ (**3**)

	x	*y*	*z*	*U*[a]
Pt	0	6275 (2)	7500	31 (1)
P(1)	421 (7)	4560 (10)	8413 (5)	41 (4)
P(2)	−90 (8)	8050 (11)	6631 (5)	47 (4)
O(1)	1177 (18)	4957 (27)	9264 (10)	55 (9)
O(2)	1104 (17)	3376 (26)	8230 (12)	57 (10)
O(3)	−490 (17)	3706 (29)	8610 (12)	62 (10)
O(4)	817 (21)	9209 (24)	7101 (14)	68 (12)
O(5)	485 (20)	7335 (24)	6096 (11)	54 10)
O(6)	−1105 (19)	8730 (32)	6160 (12)	66 (10)
C(1)	2243 (30)	5700 (48)	9429 (21)	82 (20)
C(2)	1583 (41)	2187 (44)	8682 (22)	96 (24)
C(3)	−1600 (30)	4255 (56)	8371 (25)	100 (25)
C(4)	1040 (38)	10361 (41)	6790 (26)	95 (25)
C(5)	160 (35)	7698 (54)	5348 (20)	90 (23)

[a] Equivalent isotropic *U* defined as one-third of the trace of the orthogonalized U_{ij} tensor.

(24) Shustorovich, E. *J. Am. Chem. Soc.* **1979**, *101*, 792.
(25) Shustorovich, E. *Inorg. Chem.* **1979**, *18*, 1039.

Table V. Atomic Coordinates (×10^4) and Isotropic Thermal Parameters (Å^2 × 10^3) for $C_9H_{27}O_9P_4ClF_6Pt$ (**4**)

	x	y	z	U[a]
Pt	3838.8 (5)	1607.4 (1)	1822.7 (3)	60.9 (1)
Cl	2292 (5)	2282 (1)	1988 (3)	105 (1)
P(1)	4174 (4)	1875 (1)	−3 (3)	82 (1)
P(2)	5561 (4)	1007 (1)	1744 (2)	66 (1)
P(3)	3265 (4)	1383 (1)	3629 (3)	83 (1)
P(4)	9265 (5)	630 (1)	7231 (3)	98 (1)
F(1)	7279 (13)	538 (5)	6887 (15)	256 (8)
F(2)	9111 (23)	935 (5)	8203 (13)	315 (11)
F(3)	9084 (21)	1027 (5)	6435 (15)	298 (10)
F(4)	9512 (18)	222 (5)	8076 (14)	277 (9)
F(5)	11271 (13)	708 (5)	7507 (11)	212 (7)
F(6)	9572 (16)	327 (5)	6244 (12)	241 (8)
O(1)	2625 (12)	2144 (3)	−756 (7)	109 (4)
O(2)	4535 (12)	1474 (3)	−822 (7)	106 (4)
O(3)	5606 (17)	2245 (4)	15 (9)	153 (6)
O(4)	4810 (10)	591 (3)	972 (8)	106 (4)
O(5)	7174 (9)	1161 (3)	1226 (7)	93 (3)
O(6)	6387 (11)	819 (3)	2987 (6)	97 (3)
O(7)	4626 (22)	1525 (4)	4768 (9)	210 (8)
O(8)	3045 (12)	865 (3)	3696 (7)	109 (4)
O(9)	1941 (23)	1661 (5)	4203 (12)	93 (7)
O(9′)	926 (35)	1391 (11)	3319 (23)	95 (12)
C(1)	877 (19)	1937 (5)	−1068 (14)	153 (8)
C(2)	4736 (27)	1541 (5)	−2052 (12)	157 (10)
C(3)	6984 (24)	2350 (6)	907 (17)	196 (12)
C(4)	3114 (19)	456 (5)	561 (15)	159 (9)
C(5)	8434 (20)	890 (6)	829 (15)	161 (10)
C(6)	6906 (22)	362 (5)	3326 (13)	154 (8)
C(7)	6059 (20)	1752 (5)	4989 (13)	132 (7)
C(8)	2881 (22)	613 (4)	4757 (12)	138 (8)
C(9)	84 (32)	1607 (9)	3899 (38)	174 (19)
C(9′)	314 (64)	1679 (13)	3732 (32)	151 (22)

[a] Equivalent isotropic U defined as one-third of the trace of the orthogonalized U_{ij} tensor.

Table VI. Atomic Coordinates (×10^4) and Isotropic Thermal Parameters (Å^2 × 10^3) for $C_6H_{18}O_6P_2Cl_2Pt$ (**5**)

	x	y	z	U[a]
Pt	0	8933.5 (2)	2500	42.0 (1)
Cl(1)	576 (7)	7640 (2)	3181 (4)	68 (1)
Cl(2)	2676 (7)	9335 (3)	3818 (3)	69 (1)
P(1)	−465 (5)	10166 (2)	2026 (3)	44 (1)
P(2)	−2462 (5)	8474 (2)	1434 (3)	45 (1)
O(1)	1346 (21)	10746 (7)	2351 (12)	64 (4)
O(2)	−2103 (22)	10634 (10)	2452 (10)	63 (4)
O(3)	−1193 (18)	10223 (7)	865 (7)	54 (3)
O(4)	−4149 (18)	9099 (7)	1080 (12)	66 (4)
O(5)	−1900 (23)	8171 (8)	434 (8)	66 (4)
O(6)	−3557 (17)	7723 (7)	1764 (10)	60 (4)
C(1)	3100 (34)	10637 (14)	1912 (21)	80 (8)
C(2)	−2011 (29)	10655 (12)	3533 (14)	63 (6)
C(3)	−1653 (41)	11001 (10)	377 (17)	73 (7)
C(4)	−5858 (31)	8886 (12)	366 (24)	81 (8)
C(5)	−622 (28)	7529 (13)	412 (15)	70 (6)
C(6)	−4192 (42)	7698 (12)	2725 (20)	86 (9)

[a] Equivalent isotropic U defined as one-third of the trace of the orthogonalized U_{ij} tensor.

Table VII. Bond Distances (Å) Involving Pt(II) for **1–5**

	1	2	3	4	5
Pt–P(OMe)$_3$					
Pt–P(1)	2.313 (4)		2.294 (9)	2.296 (3)	2.192 (3)
Pt–P(2)	2.305 (4)	2.290 (3)		2.216 (3)	2.155 (3)
Pt–P(3)	2.311 (4)	2.306 (3)		2.301 (3)	
Pt–P(4)	2.311 (4)	2.296 (3)			
Pt–P(O)(OMe)$_2$					
Pt–P(1)		2.322 (3)			
Pt–P(2)			2.329 (10)		
Pt–Cl					
Pt–Cl(1)				2.333 (3)	2.384 (4)
Pt–Cl(2)					2.408 (4)

complexes is comparable in magnitude but not tightly correlatable. Not only are the many contributing factors in $^1J_{Pt-P}$ inadequately accounted for but also, as indicated by the structure of **5**, the Pt–P bond distances can be unexpectedly and significantly different without a simple reason.

Table VIII. Selected Bond Angles (deg) for **1–5**

	1	2	3	4	5
Pt[P(OMe)$_3$]$_2$					
P(1)–Pt–P(2)	91.1 (1)			92.4 (1)	95.5 (1)
P(1)–Pt–P(3)	173.6 (1)			174.5 (1)	
P(2)–Pt–P(3)	90.0 (1)	91.4 (1)		92.8 (1)	
P(1)–Pt–P(4)	89.7 (1)				
P(2)–Pt–P(4)	167.0 (1)	168.1 (1)			
P(3)–Pt–P(4)	90.7 (1)	91.2 (1)			
P(1)–Pt–P(1a)			90.1 (4)		
Pt[P(OMe)$_3$]-[P(O)(OMe)$_2$]					
P(1)–Pt–P(2)		88.5 (1)	169.7 (4)		
P(1)–Pt–P(3)		170.1 (1)			
P(1)–Pt–P(4)		90.9 (1)			
P(2)–Pt–P(1a)			91.8 (3)		
Pt[P(O)(OMe)$_2$]$_2$					
P(2)–Pt–P(2a)			88.2 (5)		
ClPt[P(OMe)$_3$]					
Cl–Pt–P(1)				87.2 (1)	
Cl–Pt–P(2)				174.1 (1)	
Cl–Pt–P(3)				87.8 (1)	
Cl(1)–Pt–P(1)					174.4 (1)
Cl(1)–Pt–P(2)					88.7 (1)
Cl(2)–Pt–P(1)					84.8 (1)
Cl(2)–Pt–P(2)					173.6 (1)
PtCl$_2$					
Cl(1)–Pt–Cl(2)					85.8 (1)

Table IX. Deviations (Å) from Least-Squares Planes for **1–5**

atom	deviations	atom	deviations
compound **1**:	$0.7756x + 0.5896y - 0.2254z - 6.6181 = 0$		
Pt	−0.053	P(3)	−0.182
P(1)	−0.182	P(4)	0.209
compound **2**:	$0.3412x + 0.8383y - 0.4253z - 7.2213 = 0$		
Pt	0.014	P(3)	0.211
P(1)	0.216	P(4)	−0.218
P(2)	−0.223		
compound **3**:	$0.9807x + 0.0000y - 0.1956z + 2.8105 = 0$		
Pt	0.0000	P(1a)	−0.205
P(1)	0.205	P(2a)	−0.204
P(2)	0.204		
compound **4**:	$0.8238x + 0.4850y + 0.2934z - 5.1221 = 0$		
Pt	−0.031	P(3)	−0.071
P(1)	−0.072	Cl	0.088
P(2)	0.086		
compound **5**:	$0.6250x - 0.1524y - 0.7656z + 4.9534 = 0$		
Pt	0.055	Cl(1)	−0.014
P(1)	−0.017	Cl(2)	−0.011
P(2)	−0.013		

Table X. ^{195}Pt–^{31}P Coupling Constants and Bond Distances for Pt(II)–Phosphite and Pt(II)–Phosphonate Complexes

compd	$^1J_{Pt-P}$, Hz	d(Pt–P), Å
1	3908	2.310 (7)
2	3086[a]	2.306 (3)
	4239[b]	2.293 (3)
	3488[c]	2.322 (3)
3	3260[a,b]	2.294 (9)
	3971[c]	2.329 (10)
Pt[P(OH)(OMe)$_2$][P(OMe)$_3$]$_2$	3455[d]	2.312 (3)[d]
Pt[[P(O)(OMe)$_2$]$_2$BF$_2$]$_2$	3580[e]	2.299 (2)[e]
trans-Pt(SnCl$_3$)$_2$[P(OPh)$_3$]$_2$	3930[f]	2.272 (3)[f]
4	5569[a]	2.216 (3)
	3911[b]	2.299 (3)
5	5671	2.173 (2)
cis-PtCl$_2$(PEt$_3$)[P(OPh)$_3$]	6255[g]	2.182 (2)[g]
trans-PtCl(PEt$_3$)$_2$[P(O)[OP(OEt)$_2$]$_2$]PtCl$_2$	6064[h]	2.198 (3)
PtCl[[P(O)(OMe)$_2$]$_2$BF$_2$]PEt$_3$	3880[i]	2.263 (6)[i]
	5520[c]	2.194 (5)

[a] Trans P(OMe)$_3$. [b] Cis P(OMe)$_3$. [c] P(O)(OMe)$_2^-$. [d] Reference 6. [e] Reference 9. [f] Reference 8. [g] Reference 7. [h] Reference 10. [i] Reference 11. [j] Reference 27.

Summary of Patterns in Pt(II)-Phosphite and Pt(II)-Phosphonate Complexes. 1. The lengths of the Pt-P(O)$(OMe)_2$ bonds in $Pt[P(OMe)_3]_{4-n}[P(O)(OMe)_2]_n^{(2-n)+}$, n = 1, 2, and 4, fall in the range 2.31-2.33 Å and are largely independent of the residual charge on the complex.

2. The Pt-$P(OMe)_3$ bond distance in $Pt[P(OMe)_3]_{4-n}[P(O)(OMe)_2]_n^{(2-n)+}$ complexes, n = 0, 1, and 2, fall in the range 2.29-2.31 Å, which is, on average, shorter than the Pt-phosphonate bonds.

3. On the basis of the bond distance trend, the trans influence is $P(O)(OMe)_2^- > P(OMe)_3 \gg Cl^-$. The trend for $P(OMe)_3$ and $P(O)(OMe)_2^-$ is difficult to distinguish by ^{31}P NMR spectroscopy, but the trans influence of the phosphorus ligands as a group can be easily distinguished from Cl.

4. These complexes distort away from idealized square-planar geometry by an amount that qualitatively depends on the cone angle of the ligands. The *trans*-LPtL angle order is $PtCl_4^{2-}$ (180°)[26] > *cis*-$Cl_2Pt[P(OMe)_3]_2$ (174°) ≃ $[ClPt[P(OMe)_3]]_3^+$ (174°) > $[Pt[P(OMe)_3]_4]^{2+}$ (170°) ≃ $[Pt[P(O)(OMe)_2][P(OMe)_3]_3]^+$ (169°) ≃ $Pt[P(OMe)_3]_2[P(O)(OMe)_2]_2$ (170°) > $[Pt(PMe_3)_3Cl]^+$ (166°) > $[[Pt(PEt_3)_4]]^{2+}$ (150°). If the ligands are chelated, as in $\{Pt[P(OH)_2(OMe)_2]_2[P(O)(OMe)_2]_2\}$, the distortion is less, i.e. >175°.

5. Distortion toward both square-pyramidal and tetrahedral geometry can be found at the Pt(II) center in these complexes.

6. The correlation between $^1J_{Pt-P}$ and d(Pt-P) is crude at best. It cannot be used to predict bond distances reliably from ^{31}P NMR data and vice versa.

Supplementary Material Available: Listings of bond lengths (Tables 1S, 6S, 11S, 16S, and 21S), bond angles (Tables 2S, 7S, 12S, 17S, and 22S), anisotropic thermal parameters (Tables 3S, 8S, 13S, 18S, and 23S), and hydrogen atom parameters (Tables 4S, 9S, 14S, 19S, and 24S) for **1-5** (15 pages); listings of observed and calculated structure factors (Tables 5S, 10S, 15S, 20S, and 25S) for **1-5** (102 pages). Ordering information is given on any current masthead page.

(26) Dickenson, R. G. *J. Am. Chem. Soc.* **1922**, *44*, 2404.

(27) Sperline, R. P.; Beaulieu, W. B.; Roundhill, D. M. *Inorg. Chem.* **1978**, *17*, 2030.

Contribution from the Departments of Chemistry and Nuclear Medicine, University of California, Davis, California 95616

X-ray Crystal Structure of a Macrocyclic Copper Chelate Stable Enough for Use in Living Systems: Copper(II) Dihydrogen 6-(*p*-Nitrobenzyl)-1,4,8,11-tetraazacyclotetradecane-1,4,8,11-tetraacetate

Min K. Moi,[†] Michael Yanuck,[†] Shrikant V. Deshpande,[†] Håkon Hope,[†] Sally J. DeNardo,[‡] and Claude F. Meares*[†‡]

Received December 22, 1986

With the goal of radioimmunotherapy using copper-67 attached to monoclonal antibodies, the title complex (I) has been synthesized and shown to retain the copper ion for days under physiological conditions.[10] Here we report the crystal structures of I and also of the binuclear complex dicopper(II) (6-*p*-nitrobenzyl)-1,4,8,11-tetraazacyclotetradecane-1,4,8,11-tetraacetate (II). Crystals of I are triclinic, with cell dimensions a = 8.537 (4) Å, b = 8.684 (6) Å, c = 21.614 (15) Å, α = 99.48°, β = 98.69°, and γ = 90.51°; Z = 2, and space group is $P\bar{1}$. The R value with anisotropic thermal parameters for all non-hydrogen atoms is 0.066 for 2934 reflections. In I, the Cu(II) is six-coordinate, with two axial nitrogen ligands (bond lengths 2.4 Å). The other two nitrogen atoms and two carboxylate oxygens form an approximately square plane (bond lengths 2.0 Å). Crystals of II are monoclinic, with cell dimensions a = 10.501 (3) Å, b = 9.216 (3) Å, c = 17.640 (4) Å, and β = 92.06°; Z = 2, and space group is Pc. The R value is 0.055 Å for 2650 reflections. In the binuclear complex the two coppers are pentacoordinate, and the structure is polymeric.

Introduction

The attachment of metal ions to proteins, such as monoclonal antibodies, can create new tools for use in biology and medicine.[1] The reagents used for such attachment are usually called "bifunctional chelating agents" because they incorporate a strong metal-chelating group and a chemically reactive group. Bifunctional chelating agents are most often used to endow biological molecules with the nuclear,[2] physical,[3] or chemical[4] properties of chelated metal ions. In the last few years, substantial progress has been made in the application of such reagents to problems such as cancer therapy and diagnosis,[5,6] clinical immunoassays,[7] and DNA footprinting.[8]

The properties of the chelated metal ions play a major role in the application of the bifunctional chelates. Radioisotopes of Cu, such as ^{67}Cu, have been shown to be potentially useful in radioimmunotherapy.[9] ^{67}Cu releases high-energy electrons (β particles), which can cause toxic chemical reactions to target tumor cells located within approximately 100 μm of the radionuclide. In addition, the radioactive decay of ^{67}Cu releases penetrating γ rays, which are useful for tumor imaging.

We have undertaken the development of new bifunctional chelates of ^{67}Cu that, when conjugated to antitumor monoclonal antibodies, will serve as tumor-imaging and tumor-therapeutic agents. For this application it is essential that the radioactive copper ion remain attached to the antibody for periods of several days in a living system. Copper(II) is a very labile metal ion that can exchange ligands with ease. To counteract this lability, we have prepared 6-[*p*-(bromoacetamido)benzyl]-1,4,8,11-tetraaza-

[†] Department of Chemistry.
[‡] Department of Nuclear Medicine.

(1) Meares, C. F.; Wensel, T. G. *Acc. Chem. Res.* **1984**, *17*, 202.
(2) Sundberg, M. W.; Meares, C. F.; Goodwin, D. A.; Diamanti, C. I. *Nature (London)* **1974**, *250*, 587.
(3) Leung, C. S.-H.; Meares, C. F. *Biochem. Biophys. Res. Commun.* **1977**, *75*, 149.
(4) Dreyer, G. B.; Dervan, P. B. *Proc. Natl. Acad. Sci. U.S.A.* **1985**, *82*, 968.
(5) Scheinberg, D. A.; Strand, M.; Gansow, O. A. *Science (Washington, D.C.)* **1982**, *215*, 1511.
(6) Hnatowich, D. J.; Layne, W. W.; Childs, R. L., Lanteigne, D.; Davis, M. A.; Griffin, T. W.; Doherty, P. W. *Science (Washington, D.C.)* **1983**, *220*, 613.
(7) Siitari, H.; Hemmila, I.; Sioni, E.; Lorgen, T.; Koistinen, V. *Nature (London)* **1983**, *301*, 258.
(8) Van Dyke, M. W.; Dervan, P. B. *Biochemistry* **1983**, *22*, 2373.
(9) DeNardo, S. J.; Jungerman, J. A.; DeNardo, G. L.; Lagunas-Solar, M. C.; Cole, W. C.; Meares, C. F. In *The Developing Role of Short-Lived Radionuclides in Nuclear Medical Practice*; Paras, P., Theissen, J. W., Eds.; U.S. Department of Energy: Washington, DC, 1984.

0020-1669/87/1326-3458$01.50/0